



Audio Engineering Society

Convention e-Brief 577

Presented at the 148th Convention
2020 June 2–5, Online

This Engineering Brief was selected on the basis of a submitted synopsis. The author is solely responsible for its presentation, and the AES takes no responsibility for its contents. All rights reserved. Reproduction of this paper, or any portion thereof, is not permitted without direct permission from the Audio Engineering Society.

MEMS based Audio Speaker Module

Markus Hänsler¹, Giacomo Muraro², Christian Novotny², Richard Murphy², Jakob Spötl², Andrea Rusconi Clerici²

¹ USound GmbH, Kratkystrasse 2, 8010 Graz, Austria

² USound GmbH, Gutheil-Schoder-Gasse 8-12, 1100 Vienna, Austria

Correspondence should be addressed to andrea.rusconi@usound.com

ABSTRACT

This paper introduces a novel MEMS technology based audio module for in-ear headphone applications. The device has a small form factor with the whole audio module integrated inside the tip of an in-ear headphone. It is a complete audio solution containing a surface mounted MEMS speaker, an integrated audio amplifier with energy recovery, a digital MEMS microphone as well as digital signal processing for equalization and open-loop predistortion. The module can be manufactured in an SMT line enabling fully automated high-volume mass production with low costs and high yield.

The mechanical structure and key benefits of a MEMS based speaker module are discussed in detail, along with the fundamentals of the audio amplifier implementation and signal processing.

1 Introduction

The mechanical design and assembly process of today's earbuds have become increasingly complex. This is particularly clear in applications like true wireless earbuds (TWS). These involve complex and expensive components as well as time-consuming manual assembly steps. The complexity has increased further with active noise cancelling (ANC) integration, where at least one microphone needs to be integrated into the earbud as well. This novel MEMS based digital audio module addresses these issues by providing a solderable acoustic package with a small form factor while still providing high quality audio performance. The module is developed so that it can be used off-the-shelf, saving customers from investing time and money in developing and optimizing the acoustic environment of the earbud.

2 Mechanical Structure

The mechanical concept is that the audio module sits directly in the ear canal of the user, leading to an ideal acoustic experience. The module fits standard headphone ear tips for flexible size adjustment. The body of the TWS system with battery and antenna is then built to sit inside the outer ear for good signal quality. The audio module shell creates a closed front volume for the speaker and microphone. This is ideal for rich, full-bodied sound reproduction and for high quality ANC capability. The back volume consists of the remaining space available in the TWS body. The audio module shell incorporates front venting to allow for pressure adjustment of the TWS in the ear canal. The audio module also includes a mesh for dust protection, along with a waterproof membrane for robustness and high performance.

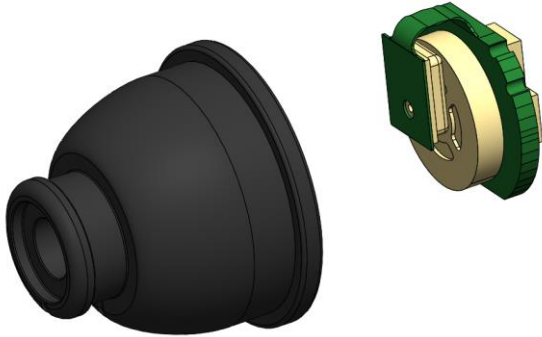


Figure 1: Audio module shell and Rigid-Flex PCB containing MEMS Speaker, amplifier for MEMS speaker and ANC feedback microphone

3 Feedback Microphone

The integration of a feedback microphone close to the front of the speaker has become the new trend in TWS design. Apple's AirPods Pro are the most prominent example, but other leading brands like Sony and Bose have products featuring this as well. Every company faces the same problems of acoustically optimal microphone placement, omitting resonance effects, while keeping the design small enough to still fit into the ear and achieve a visually appealing look. The current solutions involve manual assembly steps carefully placing and gluing the feedback microphone in front of the speaker. In the MEMS audio module the microphone and speaker are already integrated as a sub-assembly connected via Rigid-Flex PCB. A digital bottom-port MEMS microphone is used to keep the electronics package as small as possible.

4 Audio Amplifier

The audio module includes all the electronics required to drive the MEMS speaker. This consists of the audio amplifier chip plus passive components and additional circuitry. The audio module can be built with an existing off-the-shelf audio amplifier that meets the MEMS speaker requirements or with the optimized MEMS specific digital audio amplifier currently being developed. This section will discuss the optimized MEMS specific digital audio amplifier due to the unique advantages it offers (Fig. 2).

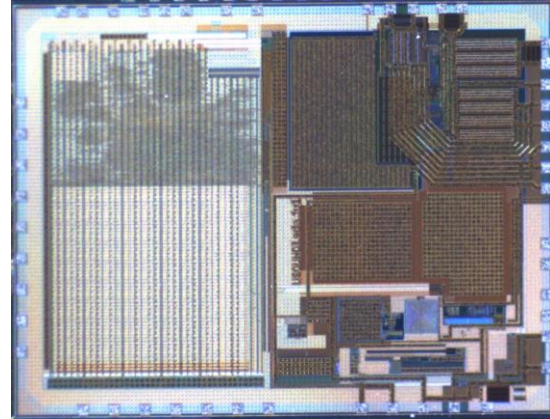


Figure 2: Silicon die microscope image of the optimized MEMS specific audio amplifier prototype.

The basic block diagram of the main audio amplifier path can be seen in Figure 3. The amplifier has an I2C interface for configuration as well as an I2S master output.

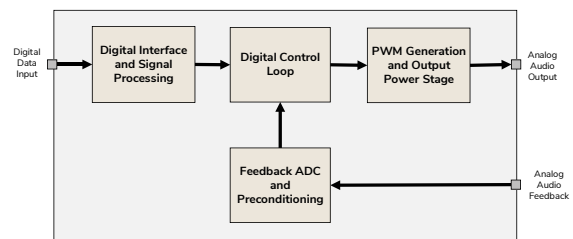


Figure 3: Audio amplifier, basic block diagram

The amplifier is a closed-loop system with digital loop control. The input for the loop control is the digital audio input signal and the digital value of the current output voltage, provided by the feedback ADC. The digital control loop sends the input signal to a pulse width modulation (PWM) stage. The required output voltage is defined by changing the pulse width. The output power stage provides the high voltage required at the speaker (up to 30 V_{PP}) and includes energy recovery functionality to reduce overall power consumption. More detailed information on the power stage and energy recovery can be found under ref. [1]. In addition to the main loop, all other required audio processing is

implemented so that no additional configuration or signal processing is needed outside the module.

There are two main use cases for the audio module implementation: standalone, and host based. With standalone operation no configuration of the audio module is needed, all settings are stored on nonvolatile memory and read by the amplifier during startup. For this type of operation only the digital audio interface and supply voltage is required to drive the audio module. With host based operation there is full flexibility for the user of the audio module to configure all important settings like digital filter settings, predistortion coefficients, DC offset voltages, and gain settings. A hybrid can also be implemented, for example one where the configuration is stored outside the audio module and is transferred to the module during start up.

An additional feature of the amplifier is the on-chip adaptive non-linearity compensation. Supported by a lookup table, all non-linearities of the system as well as variations on the load can be compensated. The lookup table can be set into an adaptive operation mode where variations during run time (for example load or temperature) can be compensated and the table can be adapted accordingly.

To improve power consumption, especially at high amplitudes, a novel energy recovery architecture is included inside the output driving stage. Figure 4 shows the current flow based on a schematic based system simulation during one sine wave period. During the rising phase of the sine wave, energy is transferred to the MEMS speaker. During the falling edge, the energy is recovered and brought back to the remaining system. The maximum peak efficiency during charging is up to 80 % and close to 70 % during discharging.

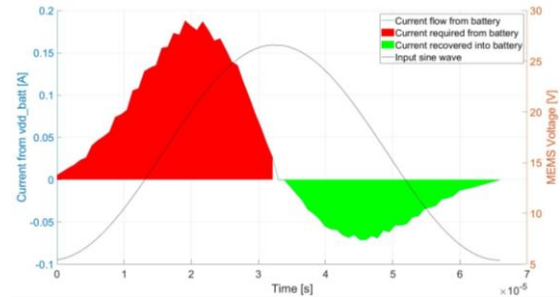


Figure 4: Current flow during one sine wave period showing energy recovery functionality [1]

5 Non-linearity and compensation

The actuators of the MEMS speaker consist of an active layer made of lead zirconate titanate (PZT), which is the piezoelectric material, and a passive silicon layer. A voltage signal is sent through the piezoelectric material, which contracts. The silicon layer constrains the adjacent PZT, and so the actuators bend. Each MEMS speaker contains six actuators which are connected to a central mass with springs. The center mass is attached to a soft elastomer membrane.

5.1 Piezoelectricity Fundamentals

The piezoelectric effect refers to the relationship between applied mechanical stress and the resulting charge generated. The piezoelectric effect is a reversible process and most of the materials that exhibit the piezoelectric effect show also the inverse effect, called converse piezoelectric effect, i.e., the generation of mechanical stress given an electric excitation. The direct piezoelectric effect is used in sensors, while the converse piezoelectric effect is used for actuators. In the piezoelectric effect the vector of the mechanical strain \vec{S} and the vector of the dielectric displacement \vec{D} are described by the constitutive piezoelectric linear equations, which can be written, using Voigt notation, as:

$$\vec{T} = c^E \vec{S} - e^t \vec{E} \quad (1)$$

$$\vec{D} = e^S \vec{S} - \epsilon^S \vec{E} \quad (2)$$

with the vector of mechanical stresses \vec{T} , the vector of the electric field \vec{E} , the tensors of the mechanical stiffness c^E (measured at constant electric field), the tensor of the piezoelectric moduli e , and the tensor of the dielectric permittivity ϵ^S (obtained at constant strain).

Equations (1) and (2) are a valid first approximation of the real behavior when the voltage signal is unipolar, i.e. when it never changes sign. A graphical explanation of typical polarization and strain loops can be seen in Figure 5 and Figure 6: Strain loop for a typical piezoelectric material Figure 6.

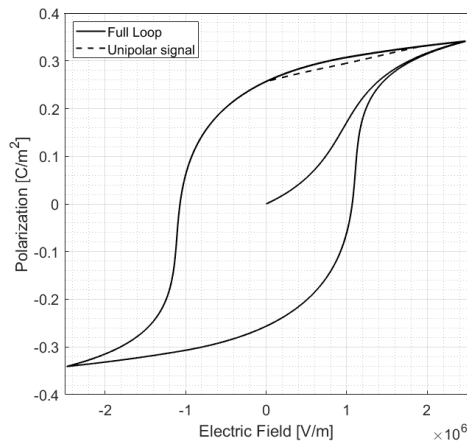


Figure 5: Polarization loop for a typical piezoelectric material

If the signal changes its sign, the polarization switches its direction in a highly nonlinear and hysteretic manner [2], following the cycle showed in Figure 5. The consequence on the strain is shown in Figure 6, with a cycle that, because of its peculiar shape, is often referred as a butterfly loop.

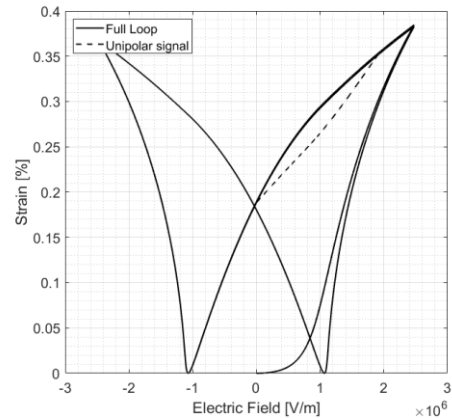


Figure 6: Strain loop for a typical piezoelectric material

However, by applying a DC offset to the signal it is possible to avoid the polarization switch. In this case, as can be seen from the small loops in Figure 5 and in Figure 6: Strain loop for a typical piezoelectric material, the system presents only small hysteretic behavior and the non-linearities are heavily reduced. Therefore, piezoelectric loudspeakers can only be driven with a DC offset combined with the desired audio signal.

5.2 Non-linearities in piezo MEMS loudspeakers

While in traditional moving coil loudspeakers the main causes of harmonic distortion are the non-linear $B \times l$ factor, the non-linear inductance of the coil, and the non-linear stiffening of the membrane, for piezoelectric MEMS loudspeakers harmonic distortion is mainly linked to the piezoelectric effect. The piezoelectric moduli e is proportional to the the state of polarization of the material [2]. Therefore, a non-constant polarization will lead to non-constant electro-mechanical coupling.

The other main root of distortion is given by the geometric nonlinearities and by the stiffening of the structure (actuators and springs) for large displacements. This effect is comparable to the non-linear K_{ms} in moving coil loudspeakers, with the peculiarity that in piezoelectric loudspeakers the DC offset shifts the low signal operation point to a point where the structure is not in the resting position.

5.3 Compensation of non-linearities

The deflection of the MEMS is proportional to the tensor of the piezoelectric moduli e , which is non-linear with respect to the electric field applied (therefore to the input voltage signal), and inversely proportional to the stiffness of the device, which is non-linear with respect to the deflection itself. This can be written as:

$$x \propto \frac{e_{31}(V)}{K(x)} V \quad (3)$$

Equation (3) can be used to model, within a good approximation, the non-linear behavior of the speaker, and can also be used in turn to compute a linearization of the system. The non-linear factors were modelled approximating the real behavior with polynomial fits. In the same way, the compensation can also be fitted into a polynomial expansion. This method is convenient because it is easily implementable in the digital signal processing (DSP) block. Figure 7 shows the signal flow charts of the system with the main blocks being the equalization filters and the polynomial pre-distortion.

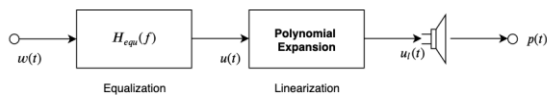


Figure 7 : Signal flow chart of the system

The effect of the compensation can be seen in Figure 8, which shows acoustic measurements of the speaker in an ear simulator (G.R.A.S 43AC Coupler), at a sound pressure level of 118.5 dB SPL at 1000 Hz. As one can see, the THD at low frequencies drops from approximately 3% to a value close to 1%. The remaining 1% is mainly linked to the fact that the polynomial compensation does not take into account the hysteretic behavior showed in Figure 5 and 6, but it only compensates a nonlinear approximation obtained by averaging the upper part with the lower part of the loop.

When compensating the hysteretic loops at the same signal, the THD decreases to values between 0.2%

and 0.4%. Nevertheless, this has not yet been implemented in the DSP.

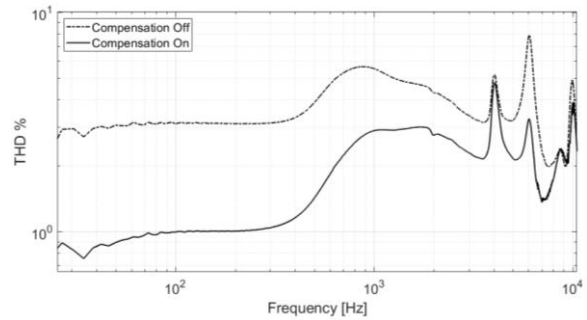


Figure 8 : Acoustic THD with and without compensation at 118.5 dB SPL

6 Conclusion

This paper shows the potential of MEMS based speaker technology to enable the development of a tiny audio module integrating all electronics for driving the speaker and performing signal processing. In addition, the performance improvements of open-loop predistortion was highlighted showing THD improvements from 3% down to 1%. This value could be further decreased down to 0.2% by also considering hysteresis effects within the predistortion.

References

- [1] M. Hänsler and M. Auer, "Design Considerations for a Digital Input MEMS Speaker Audio Amplifier with Energy Recovery," in *15th Conference on Ph.D Research in Microelectronics and Electronics (PRIME)*, Lausanne, Switzerland,, 2019.
- [2] T. Hegewald, B. Kaltenbacher, M. Kaltenbacher and R. Lerch, "Efficient modeling of ferroelectric behavior for the analysis of piezoceramic actuators," *Journal of Intelligent Material Systems and Structures*, vol. 19, no. 10, pp. 1117-1129, 2008.